*Natural Resources Research (© 2019)*
https://doi.org/10.1007/s11053-019-09512-6

*Original Paper*

# Comparison of the Ability of ARIMA, WNN and SVM Models for Drought Forecasting in the Sanjiang Plain, China

**Yuhu Zhang,[1] Huirong Yang,[2,3] Hengjian Cui,[2] and Qiuhua Chen[2]**

*Received 4 January 2019; accepted 25 June 2019*

Drought is a natural disaster that profoundly impacts all parts of the environment. Drought forecasting could provide technical support for drought risk prevention. This paper explored and compared the forecasting abilities of the autoregressive integrated moving average (ARIMA) in statistics, the wavelet neural network (WNN) and the support vector machine (SVM) in machine learning for drought forecasting in the Sanjiang Plain, China. The models used in this paper are based on the standard precipitation evapotranspiration index (SPEI) on the 12-month timescale. The SPEI was calculated using precipitation and temperature data collected during the period 1979–2016 from seven meteorological stations in the study area. Then, the SPEI series were predicted with the ARIMA, WNN and SVM models separately. The coefficient of determination ($R^2$), mean-squared error (MSE), Nash–Sutcliffe efficiency coefficient (NSE) and Kolmogorov–Smirnov (K–S) distance, which is a nonparametric measure, were used to evaluate the performance of all models. A comparison between the raw data and predictions illustrates that the $R^2$ and NSE values of the WNN model were 0.837 and 0.831, respectively; those of the SVM model were 0.833 and 0.827, respectively; and those of the ARIMA model were both $> 0.9$. Moreover, the ARIMA model had smaller MSE and K–S distance values than those of the other two models. Further, analysis of variance showed that the ARIMA model exhibited an obvious advantage over the other two models when forecasting drought in the Sanjiang Plain, China. Therefore, the method used for drought forecasting depends not only on the object of the data series but also on the underlying concepts of the models or algorithms and is a choice that should be made with caution.

**KEY WORDS:** Drought forecasting, ARIMA, WNN, SVM, Sanjiang Plain.

## INTRODUCTION

Precipitation and temperature are very important natural variables or elements, and several studies indicated that they are the vital factors of drought intensity (Easterling et al. 2007; Sun and Ma 2015). The frequency and severity of droughts caused by precipitation and climate change, which are increasing worldwide, will lead to property damage and even life-threatening conditions (Pandey et al. 2019). In addition, unlike aridity, which is a permanent climatic characteristic, drought is a temporary aberration (Ndehedehe et al. 2016; Zhang and Lin 2016). China has suffered long and serious droughts, and frequent droughts in various regions have led to severe economic losses over the past several decades due to increased temperature and

[1]College of Resources Environment and Tourism, Capital Normal University, Beijing 100048, China.
[2]School of Mathematical Sciences, Capital Normal University, Beijing 100048, China.
[3]To whom correspondence should be addressed; e-mail: 18234105830@163.com



Published online: 03 July 2019

reduced precipitation (Yao et al. 2017; Zhang et al. 2017). Thus, it is important and critical to predict drought occurrence before its onset (Zhao et al. 2016). Although drought forecasting is a controversial topic with high complexity and enormous uncertainties (Durbach et al. 2017), drought forecasting studies are crucial for providing valuable information for drought risk reduction. Thus, a considerable amount of recent research has focused on predicting changes in precipitation and drought (Roundy et al. 2014).

Increasingly, more models and algorithms have been studied in previous works. Bierkens et al. (2001) developed a regionalized version of an autoregressive exogenous (ARX) time-series model, which relates the temporal variation of water table depth at a single location to a time series of precipitation surplus. This relationship has been verified to be more generally applicable. Emmanouil (2016) used the means of the Kalman filter adaptation algorithm (KFAA) to estimate the parameters of the ARX model, and the results were validated against data reported by local authorities. Giustolisi and Savic (2006) described an improved regression methodology for creating polynomial models that overcome shortcomings in computational performance, the number of tuned evolutionary parameters and complexity, and demonstrated its superiority in interpolating data and scientific knowledge. Additionally, the use of data-driven models has become a popular topic in the drought forecasting field. Of these models, the stochastic autoregressive integrated moving average (ARIMA) model is a traditional time-series model with a mathematical formula (see ''ARIMA Model'' section), and it has been widely applied to various research topics. Additionally, artificial neural networks (ANNs) and support vector machine (SVM), which are machine learning (ML) techniques, are favored by an increasing number of scholars due to their excellent and efficient algorithms. Both ANN and SVM have been applied increasingly to a wide variety of topics. Specifically, many previous studies have shown that these two algorithms are effective for drought forecasting in specific study areas (Shin et al. 2006; Mishra et al. 2007; Tiwari and Chatterjee 2011; Djerbouai and Souag-Gamane 2016; Zhang et al. 2017). For example, Belayneh et al. (2014) reported that ANN and wavelet support vector regression (SVR) models performed with high accuracy in drought forecasting in the Awash River Basin in Ethiopia. Djerbouai and Souag-Gamane (2016) executed ANN and traditional stochastic ARIMA models in the Algerois Basin in North Algeria and showed that the ANN model was more accurate than the ARIMA model and that the coupled wavelet ANN model was the best model for drought forecasting. A similar result in the northern Haihe River Basin in China was found by Zhang et al. (2017). All of these studies have greatly contributed to their own study areas and demonstrated the superiority of neural networks and SVM methods in these cases. However, whether these two techniques, which have become increasingly prevalent in drought prediction, are more precise than the ARIMA model remains unclear. As Makridakis et al. (2018) mentioned, the majority of published studies provide forecasts and claim satisfactory accuracies without any empirical proof of their findings.

The standard precipitation evapotranspiration index (SPEI) has been proven to be an ideal tool for use in characterizing drought severity (Xiao et al. 2016) and is widely applied in drought analyses and assessments (Li et al. 2015). In a previous study, the SPEI over a 12-month timescale adequately reflected the inter-annual drought patterns when used as the drought forecast index (Guo et al. 2018).

The present study attempts to explore two different ML methods, namely wavelet neural network (WNN) and SVM algorithms, as well as traditional stochastic ARIMA models, and compare their performances in drought forecasting in the Sanjiang Plain, China. The results are evaluated using four parametric and nonparametric measures, as well as analysis of variance (ANOVA). The paper is organized as follows: ''Introduction'' section briefly reviews published studies and presents the origin of our research. ''Methods'' section provides a brief description of the methods, including the ARIMA, WNN and SVM methods used as data-driven forecasting models, as well as the performance measurement indices used to assess the accuracies of fitting of the models. ''Study Area and Data'' section introduces the study area and data sources. ''Results and Discussion'' section presents the results and a discussion in detail, followed by the conclusions in ''Conclusion'' section.

## METHODS

The technological roadmap of this paper is shown in Figure 1.

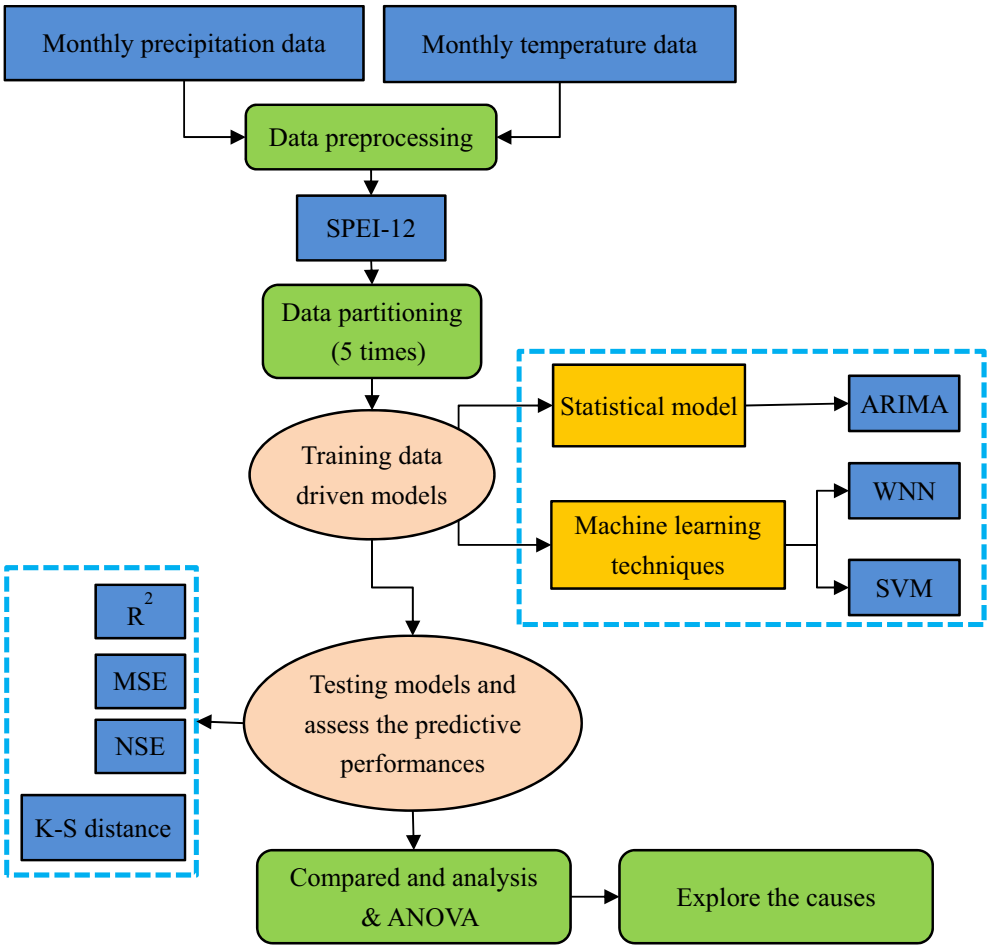


**Figure 1.** Technological roadmap of the paper.

## ARIMA Model

The autoregressive moving average (ARMA) model, which was proposed by Box and Jenkins (1976), is the most common and direct modeling method for analyzing time series. The basic idea of the ARMA model is that the sequence formed by variations over time is random, that is, a set of random variables that lie on time $t$ is considered. This sequence can be described approximately by using a corresponding mathematical model in which the occurrence of a single sequence value is uncertain but the whole sequence varies regularly. The ARMA model is formed by effectively combining the autoregressive (AR) model with a moving average (MA) model. These models can be applied directly to stationary data. Otherwise, non-stationary data must be dealt with via differential processing. Then, the ARMA model can be established, which is referred to as the ARIMA model. In general, the ARMA model after differentiation is called ARIMA $(p, d, q)(P, D, Q)_s$, in which $(p, d, q)$ is the non-seasonal part of the model and $(P, D, Q)$ is the seasonal part of the model. The ARIMA model is then given by:

$$\phi_p(B)\Phi_P(B^s)\nabla^d\nabla_s^D Y_t = \theta_q(B)_Q(B^s)e_t \quad (1)$$

The expressions in Eq. 1 are defined as follows (Djerbouai and Souag-Gamane 2016):

$$\phi_p(B) = (1 - \phi_1 B - \phi_2 B^2 - \cdots - \phi_p B^p) \quad (2)$$

$$\Phi_P(B^s) = (1 - \Phi_s B^s - \Phi_{2s} B^{2s} - \cdots - \Phi_{Ps} B^{Ps}) \quad (3)$$

$$\theta_q(B) = (1 - \theta_1 B - \theta_2 B^2 - \cdots - \theta_q B^q) \quad (4)$$

$$_Q(B^s) = (1 -_s B^s -_{2s} B^{2s} - \cdots -_{Qs} B^{Qs}) \quad (5)$$

$$B^k Y_t = Y_{t-k} \quad (6)$$

$$\nabla^d = (1 - B)^d \quad (7)$$

$$\nabla_s^D = (1 - B^s)^D \quad (8)$$

where $\phi_p(B)$ and $\theta_q(B)$ represent the non-seasonal AR and MA operators of orders $p$ and $q$, respectively; $\nabla^d$ is the difference operator that makes the data stationary; and $d$ is the value of the difference. Similarly, $\Phi_P(B)$, $_Q(B)$, $P$, $Q$, and $\nabla_s^D$ are the symbols of seasonal elements. $B$ is called the backshift operator.

The selection and estimation of parameters $p$, $q$, $P$ and $Q$ are based on the autocorrelation function (ACF), partial autocorrelation function (PACF) and Akaike information criterion (AIC). The mathematical formulation of the AIC is expressed as (Akaike 1974):

$$\mathrm{AIC} = -2 \log L + 2m \quad (9)$$

where $L$ is a monotone decreasing function of the sum of squares of the residuals of the ARIMA model called the likelihood function, and $m = (p + q + P + Q)$ denotes the number of parameters that need to be estimated in the model.

The ARIMA model is very simple and is essentially an overall linear autoregressive model that requires only endogenous variables and does not require other exogenous variables. However, the ARIMA model essentially captures only linear relationships, not nonlinear relationships (Liu et al. 2012). In other words, the data are required to be stationary. For non-stationary data, differentialization is required, but in that process, numerical information is inevitably lost.

## WNN Model

An ANN, which is a distributed parallel information processing algorithm, has self-learning, adaptability, robustness, fault tolerance and generalization characteristics (Maier et al. 2010). A wavelet packet has time–frequency and multiresolution features. A WNN, which fully combines the advantages of an ANN and wavelet packet, is based on the back-propagation (BP) neural network topology with the wave basis function as the transfer function of the hidden layer node. In a WNN, the signal is propagated forward, while the error is propagated backward.

Suppose that the input signal sequence is $x_i$ ($i = 1, 2, \ldots, k$) and the implicit layer output calculation formula is defined as:

$$h(j) = h_j \left[ \frac{\sum_{i=1}^{k} \omega_{ij} x_i - b_j}{a_j} \right] \quad j = 1, 2, \ldots, l \quad (10)$$

where $h(j)$ is the output value for the $j$th node of the hidden layer; $h_j$ is the wavelet basis function; $\omega_{ij}$ is the weight of the input layer to the hidden layer; and $b_j$ and $a_j$ are the translation and scale factors of the wavelet basis function, respectively.

In this research, the Morlet wavelet was selected as the mother wavelet (Belayneh et al. 2014; Ghosh et al. 2016), whose mathematical formula is:

$$y = \cos(1.75x)\, \mathrm{e}^{-x^2/2} \quad (11)$$

Usually, when analyzing a time series, smooth and continuous wavelet amplitudes are desired; thus, a non-orthogonal wavelet function is more suitable than an orthogonal function. In addition, to obtain information pertaining to both the amplitude and phase of the time series, a complex wavelet is chosen because it has an imaginary part; thus, the phase can be adequately expressed (Torrence and Compo 1998). The Morlet wavelet is non-orthogonal and has exponentially complex wavelets that have been adjusted by a Gaussian function. The calculation formula for the output layer is given by:

$$y(k) = \sum_{i=1}^{l} \omega_{ik} h(i) \quad k = 1, 2, \ldots, m \quad (12)$$

where $\omega_{ik}$ is the weight between the hidden layer and output layer; $h(i)$ is the output value for the $i$th hidden layer node; and $l$ and $m$ are the number of nodes of the hidden and output layer, respectively.

In addition, the gradient correction method was used to correct the wavelet basis function parameters and network weights to minimize the sum of the squared errors and make the forecast output close to the expected output. The following steps were involved in the training phase of the WNN (Ghosh et al. 2016):

1. Initialize translation factor $b_j$, scale factor $a_j$ and connecting weights $\omega_{ij}$ and $\omega_{jk}$ randomly and establish the learning rate $\eta$.
2. Input the training pair into WNN and compute the prediction and the error $e$.
3. Update the weights of the network and parameters of the mother wavelet function according to error $e$ such that the prediction of the network will approach the actual values.
4. Repeat steps 2 and 3 until convergence is achieved.

The biggest advantage of WNN over other modeling techniques is that they can model complex nonlinear processes without assuming the relationship between input and output variables (Giustolisi and Savic 2006). However, the principal disadvantages of model construction by WNN are parameter estimation and over-fitting problems. That is, WNN requires a priori identification of the structures of neural networks such as the transfer functions and the number of hidden layers (Giustolisi and Laucelli 2005).

## SVM Model

In the ML field, SVM is a supervised learning model that is typically used for pattern recognition, classification and regression analysis. SVM is based on the statistical learning theory and the assumption of structural risk minimization, and the goal of an SVM is to minimize the experience risk and confidence interval of the ML algorithm, thus allowing for good generalization (Sujay and Paresh 2014). As an algorithm type that has been proven to be robust and efficient, SVM has been extensively applied in many professions.

Considering the dataset $\{(x_1, y_1), \ldots, (x_n, y_n)\}$, the SVM focuses on finding a function that represents the relationship between $x$ and $y$, and once a new $x$ is given, this function can obtain the corresponding prediction value. The formula for the function is defined as:

$$f(x) = \sum_{i=1}^{n} w\phi(x) + b \tag{13}$$

where $w$ and $b$ are the factors used to select a linear hyperplane and represent the ultimate goals of SVM research and $\phi(x)$ defines the nonlinear mapping of $x$. When the relationship between $x$ and $y$ is not linear, $x$ can be mapped to a new space. The relationship between $\phi(x)$ and $y$ is linear in the new space. The goal of the SVM is to minimize the expected risk, which can be written as:

$$R = \frac{1}{n}\sum_{i=1}^{n} L_{\varepsilon}(y_i, f(x_i)) \tag{14}$$

where $L_\varepsilon$ is the $\varepsilon$-insensitive loss function and is expressed as (Sujay and Paresh 2014):

$$L_{\varepsilon}(y, f(x)) = \begin{cases} 0, & \text{if } |y - f(x)| \le \varepsilon \\ |y - f(x)| - \varepsilon, & \text{otherwise} \end{cases} \tag{15}$$

The target of the SVM is to decrease the expected risk and simultaneously attempts to reduce the complexity of the model by minimizing $||w||^2$. In other words, the goal is to minimize Eq. 16 such that Eq. 17 is realized (Hu et al. 2016).

$$\frac{1}{2}||w||^2 + C\sum_{i=1}^{n}(\xi_i + \xi_i^*) \tag{16}$$

$$\begin{cases} w\phi(x) + b - y_i \le \varepsilon + \xi_i, \\ y_i - w\phi(x) - b \le \varepsilon + \xi_i^*, \end{cases} \quad \xi_i, \xi_i^* \ge 0, \quad i = 1, \ldots, n \tag{17}$$

where $\xi_i$ and $\xi_i^*$ indicate the deviation of the function $f(x)$ of the predicted and observed values, respectively, and are nonnegative slack variables.

Usually, $f(x)$ in Eq. 13 can be written as (Sujay and Paresh 2014):

$$f(x) = \sum_{i=1}^{n}(a_i^* - a_i)K(x_i, x) + b, \quad 0 \le a_i^*, a_i \le C \tag{18}$$

where $a_i^*$ and $a_i$ are Lagrangian multipliers that can be obtained by solving the problem, and $K(x_i, x_j)$ is called a kernel function and equals the inner product of $\phi(x_i)$ and $\phi(x_j)$.

The radial basis function (RBF), polynomial function and sigmoid function are the most frequently used kernel functions, and these kernel functions can be presented as:

$$K(x, z) = \exp\left(\frac{||x - z||^2}{2\gamma^2}\right) \tag{19}$$

where $\gamma$ is a parameter that must be manually set. The selection of all significant parameters greatly influences the prediction accuracy of the SVM. The combination of parameters that leads to the highest $R^{2,}$ value and the lowest MSE values of the calibration dataset are ultimately selected.

The advantages of SVM algorithm are as follows: First, they are effective in high-dimensional spaces; second, they are effective in cases in which the number of dimensions is greater than the number of samples; and third, they use a subset of training points in the decision function (called support vectors), so they are also memory efficient (Decoste and Schölkopf 2002). However, if the number of features is much greater than the number of samples, an SVM is likely to perform poorly (Hu et al. 2016).

### Standard Precipitation Evapotranspiration Index (SPEI)

The SPEI measures the degree of deviation from the average state of precipitation and potential evapotranspiration, and it is used to define and monitor drought severity. The ability of the SPEI to more intuitively reflect the duration and intensity of drought has been verified (Zhang et al. 2017). Additionally, other indices, such as the Palmer drought severity index (PDSI) and the standardized precipitation index (SPI), can be applied to observe, predict and assess the severity of drought. However, the SPEI was selected as the drought index in this study because it is a combination of the PDSI and SPI, i.e., it incorporates the sensitivity of the PDSI to changes in evapotranspiration as well as the simple calculation and multiple timescale coverages of the SPI (e.g., 3 months and 12 months). Generally, the SPEI is a powerful and flexible index. Only the SPEI of the 12-month timescale was adopted in this research because it can adequately reflect inter-annual drought patterns and is sufficient for this research. Moreover, the SPEI indicates the severity and probability of droughts, that is, negative values illustrate dry conditions, while positive values signify humid conditions (Barker et al. 2016; Guo et al. 2018). The computational details of the SPEI are available in the study of Vicente-Serrano et al. (2010), and Table 1 provides the drought classification based on this index.

**Table 1.** Drought Classification of SPEI

| SPEI Value | Drought Class |
|---|---|
| SPEI > 2.0 | Extremely wet |
| 1.5 < SPEI ≤ 2 | Very wet |
| 1.0 < SPEI ≤ 1.5 | Moderately wet |
| − 1.0 < SPEI ≤ 1.0 | Near normal |
| − 1.5 < SPEI ≤ − 1.0 | Moderately dry |
| − 2.0 < SPEI ≤ − 1.5 | Severely dry |
| SPEI ≤ − 2.0 | Extremely dry |

### Description of the Evaluation Index

The $R^2$ (Belayneh et al. 2014), MSE (Liu et al. 2012), Nash–Sutcliffe efficiency coefficient (NSE) (Djerbouai and Souag-Gamane 2016) and Kolmogorov–Smirnov (K–S) distance (Zhang et al. 2017) were utilized to assess the predictive performances of all the aforementioned models. A specific introduction and the calculation of the K–S distance are given below.

The two-sample K–S test is a nonparametric test named after Andrey Kolmogorov and Nikolai Smirnov, and it compares the cumulative distributions of two samples and checks whether they are significantly different (Mokhtarzad et al. 2017). The advantage of the K–S test is that it is distribution-free. In other words, the K–S test does not need to pay attention to the distribution of the samples.

$$D = \max|F_1(x) - F_2(x)| \tag{20}$$

$F_1(x)$ and $F_2(x)$ denote the empirical distributions based on predicted data and observed data, respectively. The $D$ statistic is specified as the absolute maximum distance between the two cumulative distribution functions of two samples, which is called the K–S distance (Hassani and Silva 2015). The closer the value of $D$ is to 0, the greater the likelihood that the two samples originated from the same distribution.

## STUDY AREA AND DATA

The Sanjiang Plain, located in northeast China (45°01′N–48°27′56″N, 130°13′E–135°05′26″E, Fig. 2), has an area of $5.13 \times 10^4$ km$^2$. It is characterized by a temperate monsoon climate (part of the region is Dwa (hot-summer continental) and part is

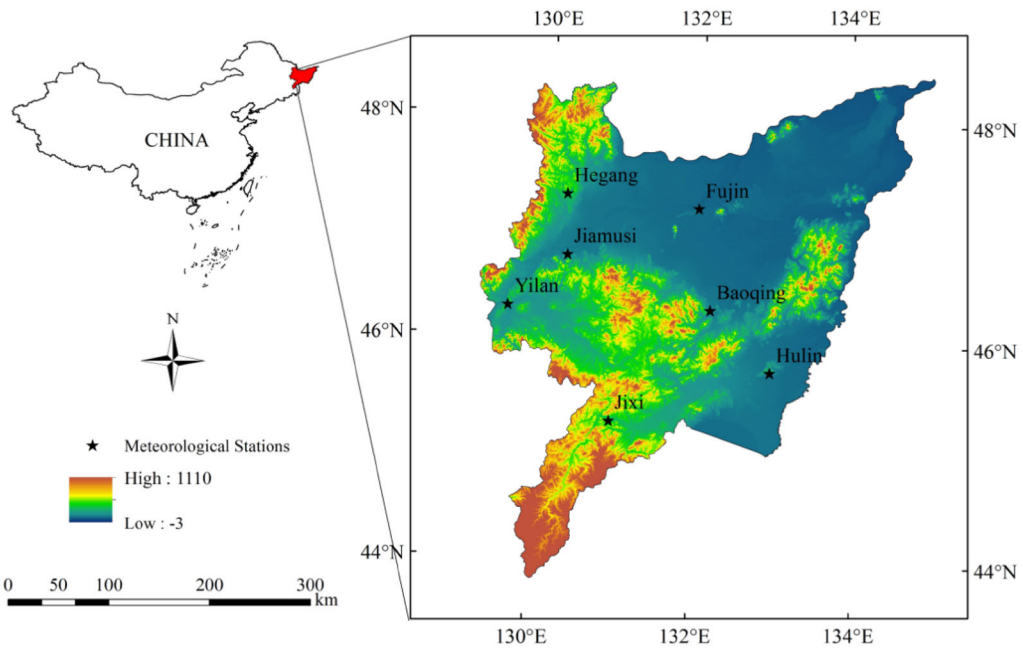


**Figure 2.** Study area and meteorological stations.

Dwb (warm-summer continental) in Koppen's climate classification) with average annual precipitation of 500–650 mm. The rainy season in the Sanjiang Plain spans from June to September, accounting for approximately 80% of the annual rainfall. The number of sunshine hours in a year ranges from 2400 to 2500 h, and the average temperature in January is − 21–18°C, while that in July is 21–22°C (Jin et al. 2016). The climate is suitable for agricultural development during the rainy and hot seasons. However, droughts have become frequent in this area in recent years, especially since 2000. Moreover, drought occurrences have approached or surpassed historical extremes because of the continuous decrease in rainfall, which has resulted in the reduction in different types of crops. Therefore, it is important to quantitatively forecast drought occurrences using model or ML methods and to analyze the applications of these methods in this region.

The monthly precipitation (mm) and temperature (°C) data from 1979 to 2016 were taken from the China Meteorological Administration (http://data.cma.cn). These data have been rigorously revised and quality controlled, including the use of contemporaneous data from neighboring sites to correct the error data and missing data and the elimination of invalid data, which ensures that the data collection time is continuous and complete and that the data availability and accuracy are close to 100%, thereby meeting the accuracy requirements of the research. Seven meteorological stations (Hegang, Fujin, Jiamusi, Yilan, Baoqing, Jixi and Hulin) were selected to represent the Sanjiang Plain, and the geographical location and basic information of the stations are listed in Table 2.

## RESULTS AND DISCUSSION

The ARIMA, WNN and SVM models for SPEI-12 are presented in this paper. In the experimental design, we split the training and testing data five times in the ratios from 80% to 90% of the training data. Table 3 shows the different splits of the training and testing data. When the models were determined to be optimal, the test dataset was forecasted using the optimal models. Then, the forecasted values and corresponding observed values, namely the original SPEI, were compared using $R^2$, MSE, NSE and K–S distance values. The averages of these values for the seven stations and the five splits in the testing data are shown in Figure 3.

## Model Development

In the following subsections, because of the difficulty presenting the results for all the five splits for all the seven stations in detail, split 1, i.e., training data during the period 1979–2008 and testing data from 2009 to 2016, is used as an example for analysis. The observed and forecasted values of the SPEI series generated by the different proposed models for each of the seven stations in the Sanjiang Plain, China, are shown in Figure 4, in which the left panel shows comparison for the training period and the right panel shows the testing period. As shown in Figure 4, the performances of the three models are comparable during both the training and general testing periods. Figure 5 shows a scatter plot of three models at seven stations, and Figure 6 shows a boxplot for the four performance indices for all stations during the testing period. The details are summarized as follows.

When significant lags of $p$ and $q$ occur in the ACF and PACF values (as shown in Fig. 7), ARIMA models were developed using different combinations, and the combination that results in the minimum AIC (Table 4) was selected as the model with the optimal fit. The results of the various performance indices of the ARIMA models at all the seven stations are presented in Table 5. During the training period, the $R^2$ and NSE values of the determinate model were greater than 0.88, and the highest value of 0.913 occurred at Jiamusi. The lowest MSE value and K–S distance value were 0.084 in Fujin and 0.029 in Hegang, respectively, during training. During the testing period, the $R^2$ and NSE values of the forecast results were greater than 0.87, with the highest values being 0.943 and 0.940 in Jixi, respectively. Moreover, the lowest MSE and K–S distance values were 0.050 in Hulin and 0.052 in Hegang and Baoqing during the testing period.

In the WNN model, the three-layer network structure that is most commonly used in meteorology (Ghosh et al. 2016) was first selected, and numbers of input neurons ranging (denoted by $P$) from 1 to 12 were tested on the basis of an ACF (left

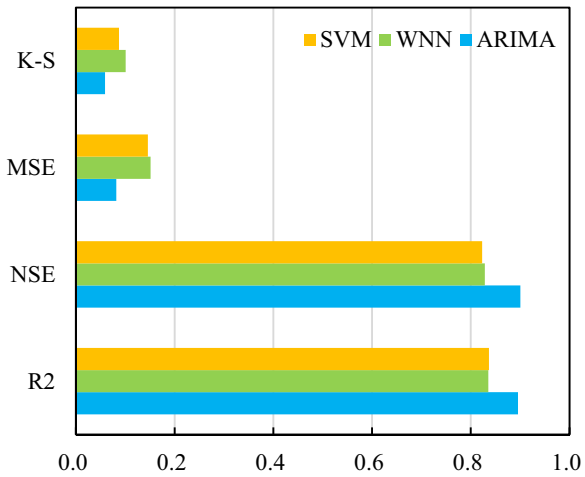


**Figure 3.** Averages of performance indices for the seven stations and five splits in the testing data.

**Table 2.** Basic information of the meteorological stations

| Site Code | Site Name | Long ($E$) | Lat ($N$) | Elevation (m) | Mean Annual Precipitation (mm) | Mean Annual Temperature (°C) |
|---|---|---|---|---|---|---|
| 50775 | Hegang | 130.30 | 47.33 | 227.90 | 640.00 | 2.80 |
| 50788 | Fujin | 132.02 | 47.23 | 66.40 | 339.50 | 3.60 |
| 50873 | Jiamusi | 130.35 | 46.83 | 81.20 | 527.00 | 3.00 |
| 50877 | Yilan | 129.55 | 46.33 | 100.10 | 555.60 | 3.30 |
| 50888 | Baoqing | 132.17 | 46.33 | 83.00 | 548.60 | 3.20 |
| 50978 | Jixi | 130.97 | 45.30 | 280.80 | 535.00 | 3.80 |
| 50983 | Hulin | 133.97 | 45.75 | 100.20 | 566.20 | 3.50 |

**Table 3.** Different data splits and the average results for the meteorological stations in the testing dataset

| Split number | 1 | 2 | 3 | 4 | 5 |
|---|---|---|---|---|---|
| Training data | 1979–2008 | 1979–2009 | 1979–2010 | 1979–2011 | 1979–2012 |
| Testing data | 2009–2016 | 2010–2016 | 2011–2016 | 2012–2016 | 2013–2016 |

## Comparison of the Ability of ARIMA, WNN and SVM Models

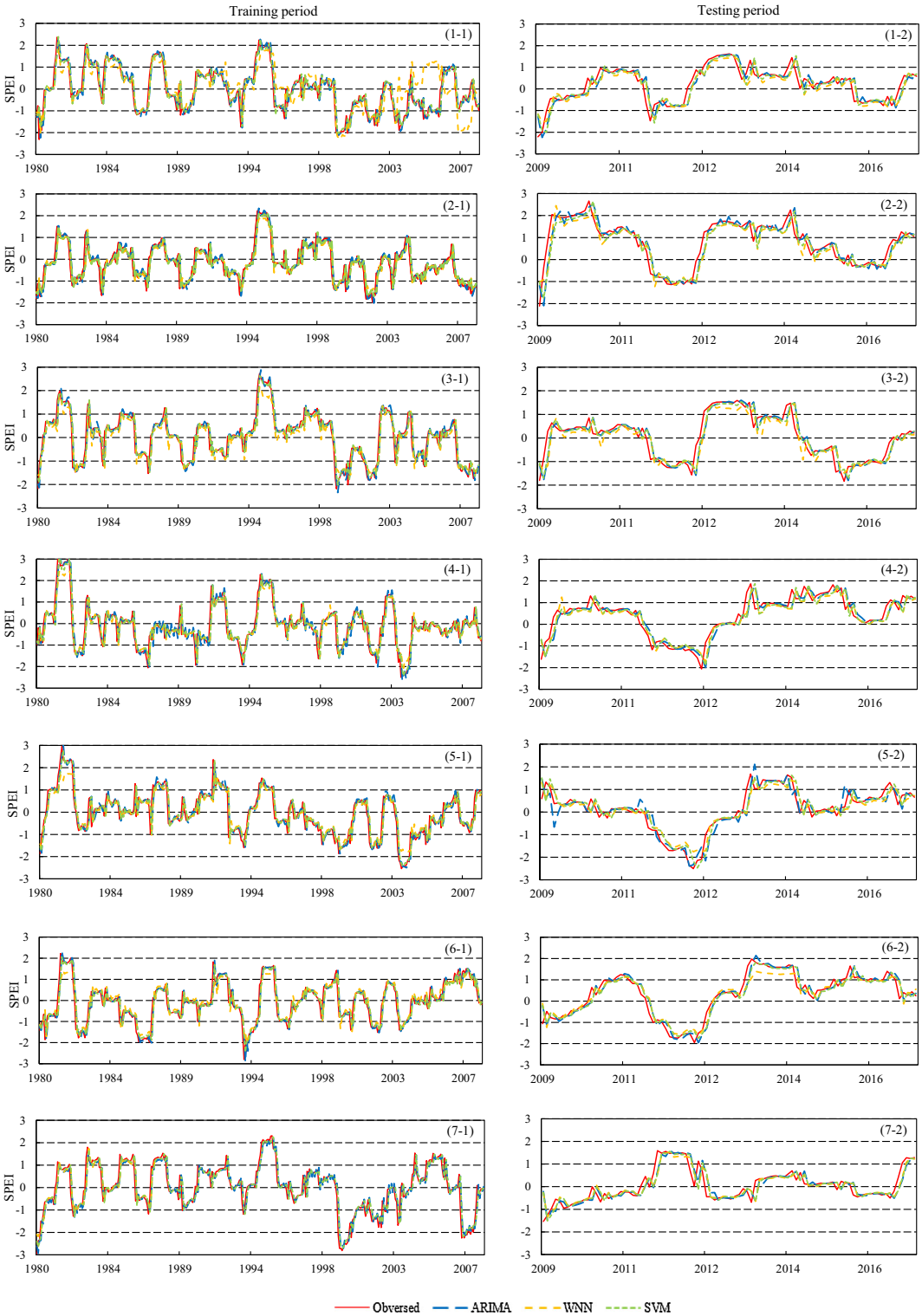


**Figure 4.** Observed vs. forecasted SPEI values for the three models during the training (left panel) and testing (right panel) periods at seven stations (1–7).

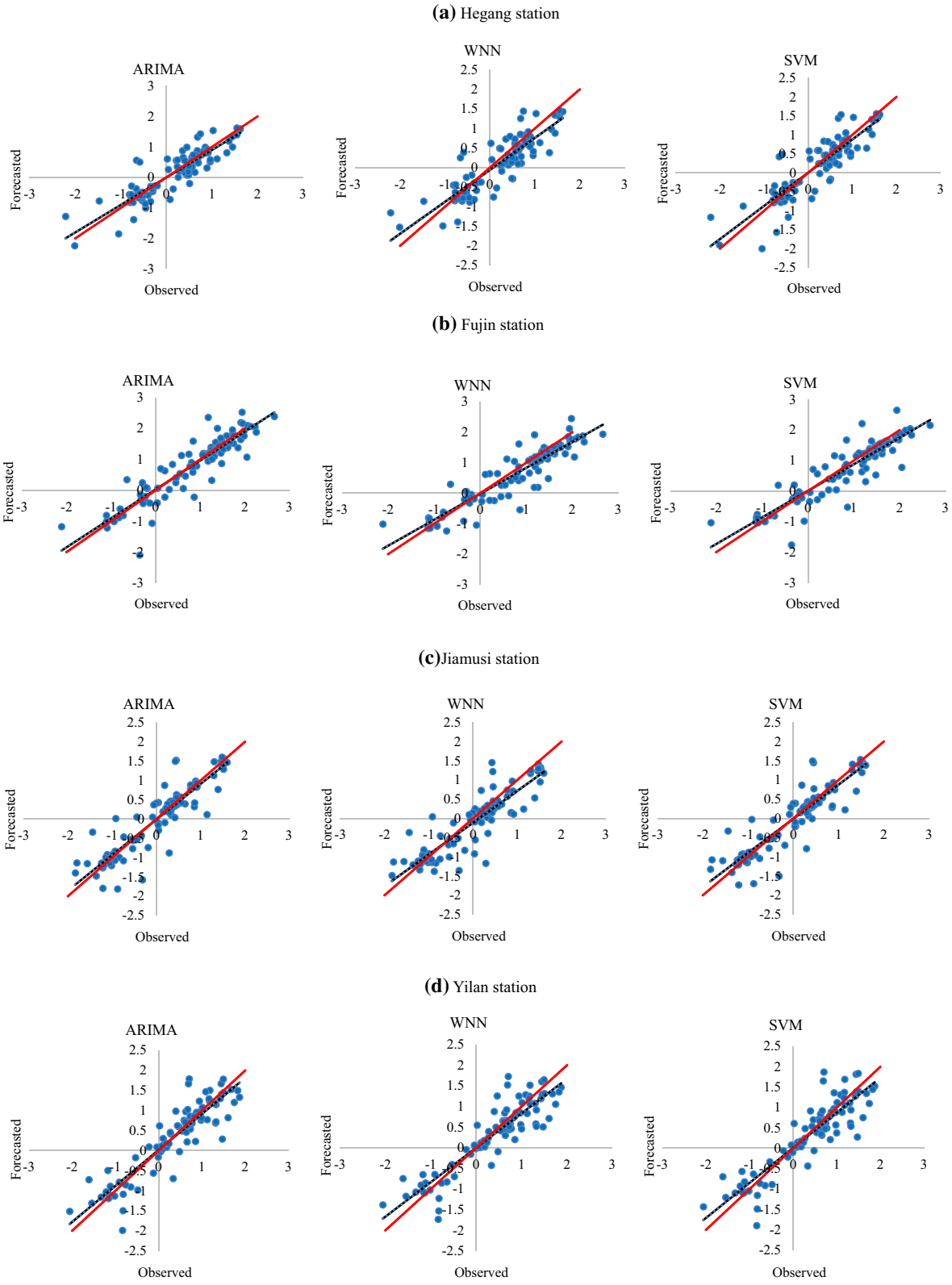


**Figure 5.** Scatter plots of the three models at seven stations.

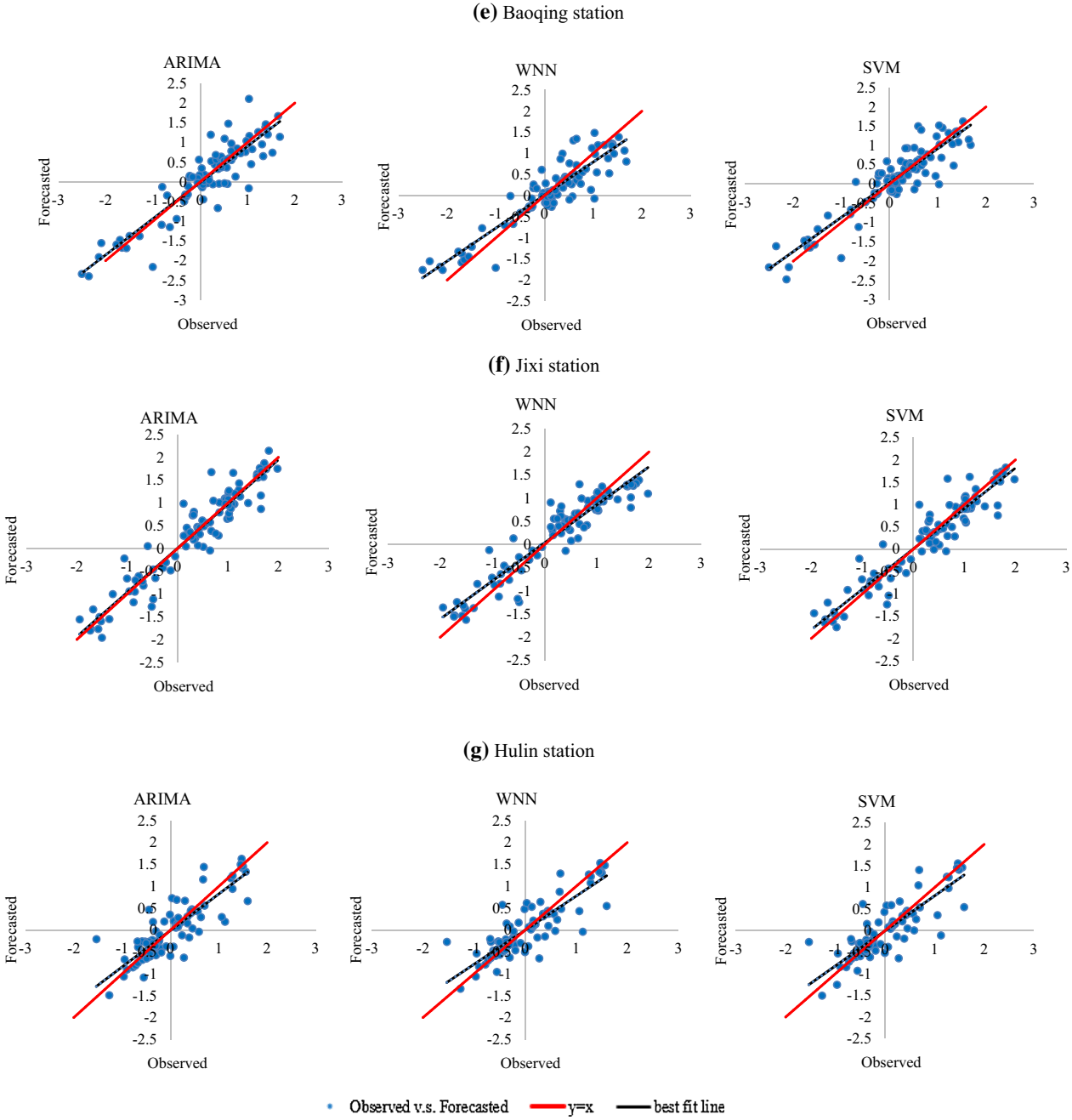


**Figure 5.** continued.

panel in Fig. 7). The number of hidden layer nodes (denoted by $Q$) was gradually increased from 4 to 8 for each input layer dimension because too few nodes cannot correctly reflect the relationship between the input and hidden variables, and too many nodes will make the network too complex, thus leading to ineffectiveness (Djerbouai and Souag-Gamane 2016). Then, the NSE and MSE between the raw and forecasted data for each combination of different $P$ and $Q$ values were computed. The combination with the best performance index was selected as the final network. The performance in-

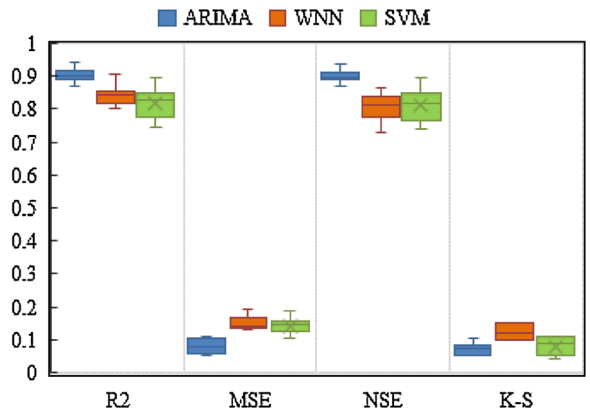


**Figure 6.** Boxplot of the four performance measures for all stations.

dices for the WNN model of the SPEI are shown in Table 6. During the training phase, the $R^2$ and NSE values of the determinate WNN model were greater than 0.79, with the highest value of 0.861 occurring in Yilan, and the lowest MSE and K–S distances values were 0.131 in Yilan and 0.061 in Baoqing and Jixi, respectively. During the testing phase, the $R^2$ and NSE values of the forecast results were greater than 0.79, with the highest values of 0.904 and 0.894 in Hulin and the lowest MSE and K–S distance values being 0.133 in Hegang and 0.098, respectively.

In the SVM model, the RBF is the kernel function, and the combination of parameters, that is, C in Eq. 16, $\varepsilon$ in Eq. 17 and $\gamma$ in Eq. 19, that resulted in the highest $R^2$ and the lowest MSE values for the calibration datasets was selected. The results of the measurements of SVM performance are presented in Table 7. During the training process, the $R^2$ and NSE values of the determinate SVM model were greater than 0.80, with the highest values being 0.864 and 0.862, and the lowest MSE and K–S distance values were 0.131 and 0.032, respectively, and all of these values occurred in Yilan. During the testing process, the $R^2$ and NSE values of the forecast results were greater than 0.79, with the highest values of 0.899 and 0.898 occurring in Hulin and the lowest MSE and K–S distance values of 0.103 and 0.043 occurring in Hulin and Jixi, respectively.

The fitting performances of the ARIMA and WNN models were compared, and the results indicated that during the training period, the ARIMA model had higher $R^2$ and NSE values and lower MSE and K–S distance values at all the seven stations. The results were similar during the testing period, such that the ARIMA model exhibited an obvious advantage, as shown in the lower parts of Tables 4 and 6. The comparison of the traditional ARIMA model with the SVM model indicated that SVM methods do not show any advantage in either the training or testing phases in terms of lower $R^2$ and NSE values and higher MSE and K–S distance values at almost all stations. Similarly, the comparison of SVM and WNN techniques clearly showed that the SVM method performed better at all sites except Fujin because the SVM had an $R^2$ value that was 0.015 lower than that of the WNN, which is a subtle difference. However, according to Figure 8, which shows the average performance results for the test sets of the seven sites, the two sites are not distinguishable and present higher $R^2$ and NSE values ($R^2$ = 0.837, NSE = 0.831) for WNN and lower MSE and K–S distance values (MSE = 0.142, K–S = 0.181) for the SVM model. Based on the average values, the traditional ARIMA model presents an $R^2$ of 0.903, an MSE of 0.080, an NSE of 0.901 and a K–S distance of 0.074. This result shows that the ARIMA model has an advantage over the WNN and SVM models in drought forecasting for the Sanjiang Plain, China. In addition, the performance indices shown in Tables 5 and 6 indicate that although the SVM model is superior during the training phase, the WNN model is slightly better during the testing stage, which is consistent with the results of Chevalier et al. (2011).

Further, ANOVA, which is useful for comparing three or more group means to identify statistically significant differences, was conducted to test whether the population means for each indicator of the three models were significantly different in this study. The results suggest that the $R^2$ and NSE values of the ARIMA model were significantly greater than those of the WNN and SVM models and that the ARIMA model had smaller MSE and K–S distance values than those of the WNN and SVM models at the 95% confidence level. In addition, significant differences were not observed between the WNN model and the SVM model at the same confidence level.

In this study, satisfactory results of drought forecast in the Sanjiang Plain were achieved based on the SPEI. The three methods all yielded good results to a certain extent (Figs. 4, 5, 6 and 8). Additionally, the accuracies of the predictions of the ARIMA model generally outperformed those of the WNN and SVM models across all evaluation indices, which illustrates that the traditional ARIMA model

## Comparison of the Ability of ARIMA, WNN and SVM Models

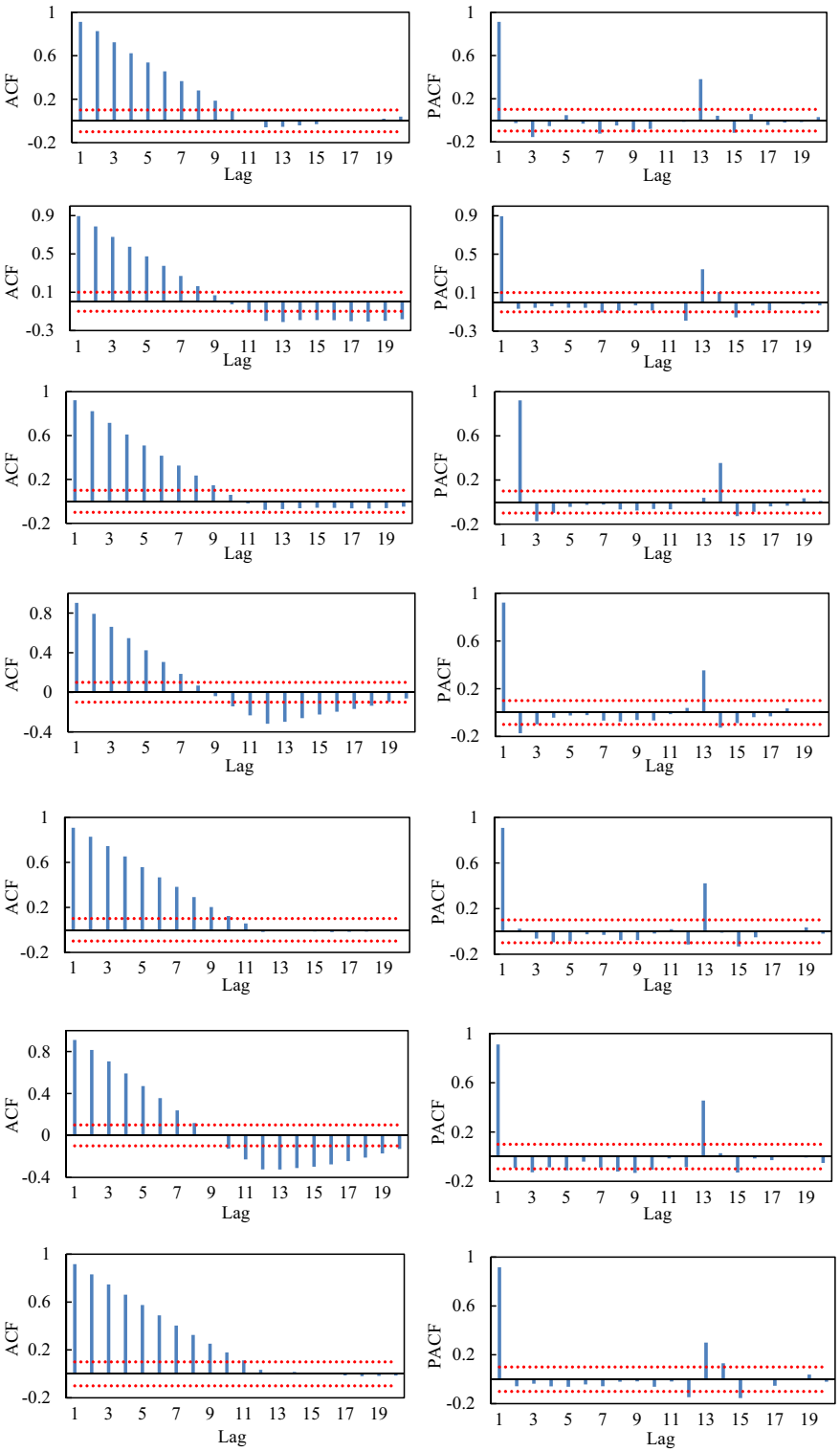


**Figure 7.** ACF (left panel) and PACF (right panel) for the SPEI series for all the seven stations.

**Table 4.** Final optimal ARIMA model

| Site name | ARIMA $(p, d, q)(P, D, Q)_s$ | AIC |
|---|---|---|
| Hegang | ARIMA $(0, 1, 0)(2, 0, 1)_{12}$ | 237.27 |
| Fujin | ARIMA $(1, 0, 0)(2, 0, 1)_{12}$ | 147.66 |
| Jiamusi | ARIMA $(1, 0, 1)(2, 0, 2)_{12}$ | 160.26 |
| Yilan | ARIMA $(1, 0, 3)(2, 0, 0)_{12}$ | 243.52 |
| Baoqing | ARIMA $(0, 1, 1)(2, 0, 0)_{12}$ | 252.96 |
| Jixi | ARIMA $(1, 0, 0)(2, 0, 2)_{12}$ | 168.11 |
| Hulin | ARIMA $(1, 0, 0)(2, 0, 2)_{12}$ | 293.37 |

is more suitable for forecasting droughts using the SPEI as a drought indicator in the Sanjiang Plain, China. Table 4 presents the final optimal ARIMA model for each station, clearly showing that the data series are stationary at the five stations because $d = 0$ and $D = 0$. Parameter $d$ is equal to 1 at only two stations (Hegang and Baoqing), which means that the data series are not stationary but vary only slightly. The information provided in "ARIMA Model" section indicates that the traditional statis-

**Table 5.** Performance Results for the ARIMA Model

| Site name | Hegang | Fujin | Jiamusi | Yilan | Baoqing | Jixi | Hulin |
|---|---|---|---|---|---|---|---|
| *Training period* | | | | | | | |
| $R^2$ | 0.890 | 0.880 | 0.913 | 0.887 | 0.883 | 0.901 | 0.890 |
| MSE | 0.110 | 0.084 | 0.086 | 0.110 | 0.115 | 0.089 | 0.127 |
| NSE | 0.889 | 0.879 | 0.913 | 0.887 | 0.882 | 0.900 | 0.890 |
| K–S | 0.029 | 0.040 | 0.037 | 0.034 | 0.037 | 0.040 | 0.052 |
| *Testing period* | | | | | | | |
| $R^2$ | 0.899 | 0.904 | 0.915 | 0.872 | 0.893 | 0.943 | 0.894 |
| MSE | 0.068 | 0.109 | 0.076 | 0.103 | 0.095 | 0.058 | 0.050 |
| NSE | 0.897 | 0.903 | 0.913 | 0.872 | 0.892 | 0.940 | 0.893 |
| K–S | 0.052 | 0.083 | 0.083 | 0.073 | 0.052 | 0.068 | 0.104 |

**Table 6.** Performance Results for the WNN Model

| Site Name | Hegang | Fujin | Jiamusi | Yilan | Baoqing | Jixi | Hulin |
|---|---|---|---|---|---|---|---|
| *Training period* | | | | | | | |
| $R^2$ | 0.820 | 0.854 | 0.802 | 0.861 | 0.808 | 0.819 | 0.806 |
| MSE | 0.200 | 0.147 | 0.140 | 0.131 | 0.189 | 0.177 | 0.191 |
| NSE | 0.818 | 0.851 | 0.797 | 0.861 | 0.807 | 0.816 | 0.800 |
| K–S | 0.072 | 0.070 | 0.071 | 0.064 | 0.061 | 0.061 | 0.099 |
| *Testing period* | | | | | | | |
| $R^2$ | 0.806 | 0.808 | 0.843 | 0.852 | 0.804 | 0.845 | 0.904 |
| MSE | 0.133 | 0.142 | 0.191 | 0.151 | 0.166 | 0.137 | 0.136 |
| NSE | 0.797 | 0.794 | 0.840 | 0.853 | 0.798 | 0.841 | 0.894 |
| K–S | 0.098 | 0.098 | 0.141 | 0.120 | 0.152 | 0.098 | 0.152 |

**Table 7.** Performance Results for the SVM Model

| Site name | Hegang | Fujin | Jiamusi | Yilan | Baoqing | Jixi | Hulin |
|---|---|---|---|---|---|---|---|
| *Training period* | | | | | | | |
| $R^2$ | 0.846 | 0.839 | 0.807 | 0.864 | 0.825 | 0.831 | 0.836 |
| MSE | 0.171 | 0.160 | 0.132 | 0.131 | 0.175 | 0.165 | 0.148 |
| NSE | 0.845 | 0.838 | 0.806 | 0.862 | 0.821 | 0.828 | 0.834 |
| K–S | 0.035 | 0.041 | 0.035 | 0.026 | 0.032 | 0.032 | 0.032 |
| *Testing period* | | | | | | | |
| $R^2$ | 0.806 | 0.806 | 0.827 | 0.829 | 0.810 | 0.851 | 0.899 |
| MSE | 0.126 | 0.146 | 0.187 | 0.148 | 0.157 | 0.130 | 0.103 |
| NSE | 0.801 | 0.798 | 0.816 | 0.825 | 0.802 | 0.849 | 0.898 |
| K–S | 0.054 | 0.065 | 0.109 | 0.087 | 0.109 | 0.043 | 0.098 |

tical ARIMA model is good at dealing with stationary data and has a formula that makes it robust when modeling the principal components of the data series. However, ML techniques, such as WNN and SVM, are better suited for strongly nonlinear data. Moreover, in theory, SVM models should have higher accuracies than those of WNN models because they adhere to the structural risk minimization principle rather than the empirical risk minimization principle, which indicates that these models should not be sensitive to local minima or maxima (Belayneh et al. 2014). The performance results of SVM and WNN models appear to be similar in the research. Moreover, previous studies have also found that the application of WNN models for time-series prediction shows comparable results to those from the use of SVM models, especially as the size of the training set increases (Witten et al. 2011). This result may be related to a lack of consideration of irrelevant attributes by the WNN models. Previous results have shown that some ML algorithms are more effective in drought forecasting (Mishra et al. 2007; Belayneh et al. 2014; Djerbouai and Souag-Gamane 2016; Mokhtarzad et al. 2017; Rhee and Im 2017); however, these phenomena occur largely independently of specific study areas without any empirical proof of the findings (Makridakis et al. 2018). Witten et al. (2011) also stated that it is almost impossible for a learning method to have universal superiority. The advantages of these methods are likely to depend on not only the basic premises of the models or algorithms but also on the object of the data series.

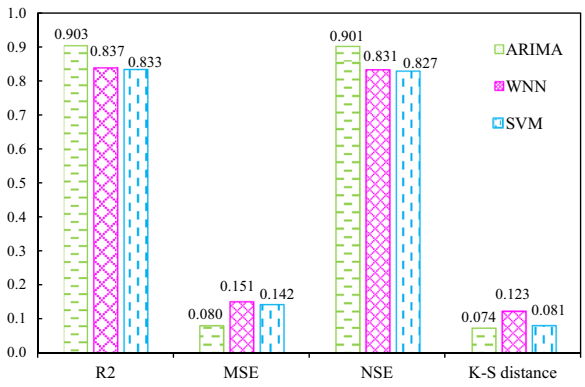


**Figure 8.** Average of each evaluation index at the seven stations for the test set.

## Sensitivity Analysis

Are the models in this paper robust, and if so, to what extent? In the following subsections, the Hegang station was used as an example for analysis.

Gaussian noise with the same $\sigma = 0.5$ and different $\mu$ was added to the SPEI series, and Figure 9 shows the comparison of the original SPEI and the noisy SPEI. Then, the SPEI with Gaussian noise is split into parts five times as shown in Table 3 and used as training and testing data for the three models. Finally, the forecasted values were compared between those from the original SPEI and those from the SPEI with Gaussian noise. The average performance results of the five splits in the test set are provided in Table 8. Additionally, Gaussian noise with the same $\mu = 0$ and different $\sigma$ was also added to the SPEI series, and Figure 10 shows the comparison of the original SPEI and this noisy SPEI. The average performance results are shown in Table 9.

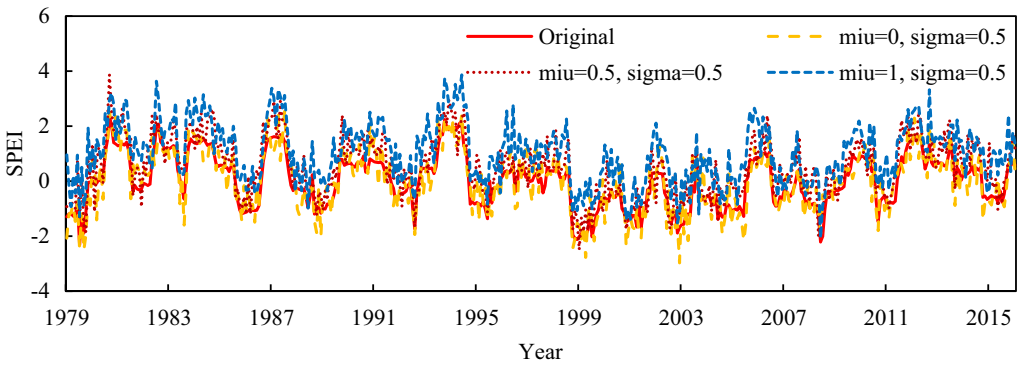


Notes: miu=μ; sigma=σ

**Figure 9.** Comparison of the original SPEI and the SPEI with Gaussian noises with the same $\sigma$ and different $\mu$.

By comparing Tables 8 and 9 with Tables 5, 6 and 7, it was found that there is no significant difference in the results before and after adding Gaussian noise. For the ARIMA model, when $\sigma = 0.5$, whether $\mu$ equals 0, 0.5 or 1, the values of $R^2$ were all stable around 0.88; the values of MSE ranged from 0.056 to 0.075; the values of NSE were between 0.874 and 0.880; and for the values of KS, the minimum was 0.023 and the maximum was 0.033. Similarly, all four performance indices for WNN and SVM were also less volatile. In addition, when $\mu = 0$, whether $\sigma$ is 0.1, 0.5 or 1, the values of $R^2$ and NSE were approximately 0.8 for the ARIMA model; the values of MSE changed between 0.113 and 0.134 for the WNN model; and for the SVM model, the values of KS ranged from 0.053 to 0.109. In other words, after adding Gaussian noise, the forecast results of the ARIMA, WNN and SVM models still remained at the original level. This result indicates that the models are robust and at least insensitive to a certain extent for the available data in this study. For these values, the errors are random and may be caused by stochastic noise. Though noise is inevitable and unavoidable, the prediction accuracy could be improved by improving the models or algorithms.

Overall, the models and algorithms could provide technical support for regional drought forecasting, and the forecast results from this study are meaningful for future research and favor preemptive development strategies to prevent drought disasters in the study area. Furthermore, drought forecasting is a complex process, and attempting these forecasts blind is not advisable. The advantages of different methods depend on both the basic premises of the models or algorithms themselves and the characteristics of the data series. It may be more reasonable and convincing to select an appropriate approach according to the characteristics of the data in different study areas. In addition, only a single model is evaluated in this paper; future studies should focus on improving the forecasting accuracy by using ensemble models or improved algorithms.

**Table 8.** Performance results for the models with Gaussian noise with the same $\sigma$ and different $\mu$

| Model | $\sigma = 0.5$ | $R^2$ | MSE | NSE | K–S |
|---|---|---|---|---|---|
| ARIMA | $\mu = 0$ | 0.882 | 0.071 | 0.879 | 0.023 |
| | $\mu = 0.5$ | 0.875 | 0.056 | 0.880 | 0.029 |
| | $\mu = 1$ | 0.870 | 0.075 | 0.874 | 0.033 |
| WNN | $\mu = 0$ | 0.807 | 0.123 | 0.801 | 0.099 |
| | $\mu = 0.5$ | 0.811 | 0.103 | 0.799 | 0.105 |
| | $\mu = 1$ | 0.799 | 0.096 | 0.798 | 0.103 |
| SVM | $\mu = 0$ | 0.798 | 0.112 | 0.802 | 0.065 |
| | $\mu = 0.5$ | 0.804 | 0.095 | 0.800 | 0.102 |
| | $\mu = 1$ | 0.800 | 0.107 | 0.789 | 0.043 |

**Table 9.** Performance results for the models with different Gaussian noise with different $\sigma$ and the same $\mu$

| Model | $\mu = 0$ | $R^2$ | MSE | NSE | K–S |
|---|---|---|---|---|---|
| ARIMA | $\sigma = 0.1$ | 0.877 | 0.072 | 0.889 | 0.056 |
| | $\sigma = 0.5$ | 0.881 | 0.069 | 0.875 | 0.064 |
| | $\sigma = 1$ | 0.875 | 0.058 | 0.881 | 0.038 |
| WNN | $\sigma = 0.1$ | 0.801 | 0.134 | 0.798 | 0.092 |
| | $\sigma = 0.5$ | 0.805 | 0.129 | 0.799 | 0.100 |
| | $\sigma = 1$ | 0.800 | 0.113 | 0.804 | 0.096 |
| SVM | $\sigma = 0.1$ | 0.800 | 0.103 | 0.797 | 0.053 |
| | $\sigma = 0.5$ | 0.802 | 0.098 | 0.800 | 0.102 |
| | $\sigma = 1$ | 0.797 | 0.125 | 0.796 | 0.109 |

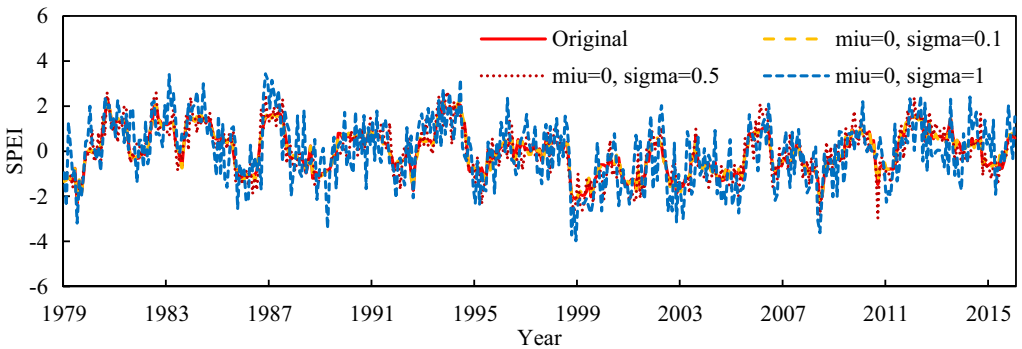


Notes: miu=μ; sigma=σ

**Figure 10.** Comparison of the original SPEI and the SPEI with Gaussian noise with different $\sigma$ and the same $\mu$.

## CONCLUSIONS

In this study, WNN, SVM and ARIMA models were used to forecast drought occurrence with the SPEI as the drought index for the period 1979–2016 in the Sanjiang Plain, China. By comparing the forecast performances of the three models, the following conclusions were obtained.

1. The ARIMA model has a significant advantage over the WNN and SVM models for drought forecasts in the Sanjiang Plain, China, according to various performance indices, namely the $R^2$, MSE, NSE and K–S distance values.
2. Comparisons of the WNN and SVM models showed that the SVM model exhibited better performance during the training period, while the WNN model was superior during the evaluation stage, which is consistent with the results indicated by Chevalier et al. (2011).
3. Accordingly, WNN and SVM, which are ML techniques, are not always superior to traditional ARIMA models in forecasting drought. Different methods may be available for different regions, and the characteristics of the data should be carefully analyzed before a forecasting model is selected.

## ACKNOWLEDGMENTS

This research was supported by the National Key Research and Development Program of China (2017YFC0406002) and the Clean Development Mechanism (CDM) Fund Grant Program of China (2014108). The authors thank the anonymous reviewers for their valuable comments and constructive suggestions for improving the paper.

## REFERENCES

Akaike, H. (1974). A new look at the statistical model identification. *IEEE Transactions on Automatic Control, 19*(6), 716–723.

Barker, L. J., Hannaford, J., Chiverton, A., & Svensson, C. (2016). From meteorological to hydrological drought using standardised indicators. *Hydrology and Earth System Sciences, 20*(6), 2483–2505.

Belayneh, A., Adamowski, J., Khalil, B., & Ozga-Zielinski, B. (2014). Long-term SPI drought forecasting in the Awash River Basin in Ethiopia using wavelet neural network and wavelet support vector regression models. *Journal of Hydrology, 508,* 418–429.

Bierkens, M. F. P., Knotters, M., & Hoogland, T. (2001). Space–time modeling of water table depth using a regionalized time series model and the Kalman filter. *Water Resources Research, 37*(5), 1277–1290.

Box, G. E. P., & Jenkins, G. M. (1976). *Time series analysis, forecasting and control.* Hoboken: Wiley.

Chevalier, R. F., Hoogenboom, G., McClendon, R. W., & Paz, J. A. (2011). Support vector regression with reduced training sets for air temperature prediction, a comparison with artificial neural networks. *Neural Computing and Applications, 20,* 151–159.

Decoste, D., & Schölkopf, B. (2002). Training invariant support vector machines. *Machine Learning, 46,* 161–190.

Djerbouai, S., & Souag-Gamane, D. (2016). Drought forecasting using neural networks, wavelet neural networks, and stochastic models, case of the Algerois Basin in north Algeria. *Water Resources Management, 30*(7), 2445–2464.

Durbach, I., Merven, B., & Mccall, B. (2017). Expert elicitation of autocorrelated time series with application to e3 (energy-environment-economic) forecasting models. *Environmental Modelling and Software, 88,* 93–105.

Easterling, D. R., Wallis, T. W. R., Lawrimore, J. H., & Heim, R. R., Jr. (2007). Effects of temperature and precipitation trends on US drought. *Geophysical Research Letters, 34*(20), 396.

Emmanouil, A. V. (2016). Modeling of temporal groundwater level variations based on a Kalman filter adaptation algorithm with exogenous inputs. *Journal of Hydroinformatics, 19*(2), 191–206.

Ghosh, S., Panigrahi, K., & Parhi, D. (2016). Performance comparison of novel WNN approach with RBFNN in navigation of autonomous mobile robotic agent. *Serbian Journal of Electrical Engineering, 13*(2), 239–263.

Giustolisi, O., & Laucelli, D. (2005). Increasing generalisation of input–output artificial neural networks in rainfall–runoff modelling. *Hydrological Sciences Journal, 50*(3), 439–457.

Giustolisi, O., & Savic, D. A. (2006). A symbolic data-driven technique based on evolutionary polynomial regression. *Journal of Hydroinformatics, 8*(3), 207–222.

Guo, H., Bao, A., Liu, T., Jiapaer, G., Ndayisaba, F., Jiang, L., et al. (2018). Spatial and temporal characteristics of droughts in Central Asia during 1966–2015. *Science of the Total Environment, 624,* 1523–1538.

Hassani, H., & Silva, E. S. (2015). A Kolmogorov–Smirnov based test for comparing the predictive accuracy of two sets of forecasts. *Econometrics, 3*(3), 590–609.

Hu, W., Yan, L., Liu, K., & Wang, H. (2016). A short-term traffic flow forecasting method based on the hybrid PSO-SVR. *Neural Processing Letters, 43*(1), 155–172.

Jin, X., Du, J., Liu, H., Wang, Z., & Song, K. (2016). Remote estimation of soil organic matter content in the Sanjiang Plain, Northest China: The optimal band algorithm versus the GRA-ANN model. *Agricultural and Forest Meteorology, 218–219,* 250–260.

Li, X., He, B., Quan, X., Liao, Z., & Bai, X. (2015). Use of the standardized precipitation evapotranspiration index (SPEI) to characterize the drying trend in southwest China from 1982–2012. *Remote Sensing, 7*(8), 10917–10937.

Liu, H., Tian, H. Q., & Li, Y. F. (2012). Comparison of two new ARIMA-ANN and ARIMA-Kalman hybrid methods for wind speed prediction. *Applied Energy, 98,* 415–424.

Maier, H. R., Jain, A., Dandy, G. C., & Sudheer, K. P. (2010). Methods used for development of neural networks for the

prediction of water resource variables in river systems, current status and future directions. *Environmental Modelling and Software, 25*(8), 891–909.

Makridakis, S., Spiliotis, E., & Assimakopoulos, V. (2018). Statistical and Machine learning forecasting methods: Concerns and ways forward. *PLoS ONE, 13*(3), e0194889.

Mishra, A. K., Desai, V. R., & Singh, V. P. (2007). Drought forecasting using a hybrid stochastic and neural network model. *Journal of Hydrologic Engineering, 12*(6), 626–638.

Mokhtarzad, M., Eskandari, F., Vanjani, N. J., & Arabasadi, A. (2017). Drought forecasting by ANN, ANFIS, and SVM and comparison of the models. *Environmental Earth Sciences, 76,* 729.

Ndehedehe, C. E., Awange, J. L., Corner, R. J., Kuhn, M., & Okwuashi, O. (2016). On the potentials of multiple climate variables in assessing the spatio-temporal characteristics of hydrological droughts over the Volta Basin. *Science of the Total Environment, 557–558,* 819–837.

Pandey, P. K., Tripura, H., & Pandey, V. (2019). Improving Prediction accuracy of rainfall time series by hybrid SARIMA–GARCH modelling. *Natural Resources Research, 28*(3), 1125–1138.

Rhee, J., & Im, J. (2017). Meteorological drought forecasting for ungauged areas based on machine learning: Using long-range climate forecast and remote sensing data. *Agricultural and Forest Meteorology, 237–238,* 105–122.

Roundy, J. K., Ferguson, C. R., & Wood, E. F. (2014). Impact of land-atmospheric coupling in CFSV2 on drought prediction. *Climate Dynamics, 43,* 421–434.

Shin, K. S., Lee, T. S., & Kim, H. J. (2006). An application of support vector machines in bankruptcy prediction model. *Expert Systems with Applications, 28*(1), 127–135.

Sujay, R. N., & Paresh, C. D. (2014). Support vector machine applications in the field of hydrology: A review. *Applied Soft Computing Journal, 19,* 372–386.

Sun, C., & Ma, Y. (2015). Effects of non-linear temperature and precipitation trends on Loess Plateau droughts. *Quaternary International, 372,* 175–179.

Tiwari, M. K., & Chatterjee, C. (2011). A new wavelet-bootstrap-ANN hybrid model for daily discharge forecasting. *Journal of Hydroinformatics, 13*(3), 500–519.

Torrence, C., & Compo, G. P. (1998). A practical guide to wavelet analysis. *Bulletin of the American Meteorological Society, 79*(1), 61–78.

Vicente-Serrano, S. M., Beguería, S., & López moreno, J. I. (2010). A multi-scalar drought index sensitive to global warming: The standardized precipitation evapotranspiration index. *Journal of Climate, 23*(7), 1696–1718.

Witten, I. H., Frank, E., & Hall, M. A. (2011). *Data mining: Practical machine learning tools and techniques* (3rd ed.). San Francisco: Margan Kaufmann.

Xiao, M., Zhang, Q., Singh, V. P., & Liu, L. (2016). Transitional properties of droughts and related impacts of climate indices in the Pearl River basin, China. *Journal of Hydrology, 534,* 397–406.

Yao, N., Li, Y., Lei, T., & Peng, L. (2017). Drought evolution, severity and trends in mainland China over 1961–2013. *Science of the Total Environment, 616–617,* 73–89.

Zhang, Y., Li, W., Chen, Q., Pu, X., & Xiang, L. (2017). Multimodels for SPI drought forecasting in the north of Haihe River Basin, China. *Stochastic Environmental Research and Risk Assessment, 31*(10), 2471–2481.

Zhang, T., & Lin, X. (2016). Assessing future drought impacts on yields based on historical irrigation reaction to drought for four major crops in Kansas. *Science of the Total Environment, 550,* 851–860.

Zhao, J., Xu, J., Xie, X., & Lu, H. (2016). Drought monitoring based on TIGGE and distributed hydrological model in Huaihe River Basin, China. *Science of the Total Environment, 553,* 358–365.